A Proposed Design, Implementation and Control of Doubly Fed Switched Reluctance Motor

Eid Gouda, and M. Salah H.

***Abstract*—In this paper, rotor of switched reluctance motor (SRM) is employed by mounting copper windings on the rotor poles as well as the stator poles. Rotor and stator windings are excited from DC supply in order to increase the developed electro-magnetic torque; thus enhancing the output power of the drive and keeping the system compactness. Furthermore, the proposed SRM offers higher reliability than conventional one, if excitation of rotor windings is lost, the drive will turn into a conventional SRM, the drive will continue running as a conventional SRM. Finite element method magnetics (FEMM) software is applied to obtain the magnetic characteristics of the proposed SRM. A control strategy for excitation of rotor and stator windings is presented. MATLAB/Simulink modeling of the proposed SRM is given and validated by practical experiment. Experimental Results on a prototype show that the proposed SRM is capable of achieving an increased torque compared with conventional SRM drive.**

***Index Terms*— Doubly Fed SRM, SRM Control, Wounded Rotor.**

I. Introduction

Invention of switched reluctance motor (SRM) goes back to 1842, it consists of laminated salient stator and salient rotor. Applications of SRM drive can be found in robotics, textiles industries, electric vehicles, aerospace and industrial drives. SRM drive offers various merits because of its simple construction, highly starting torque and fast response. In addition to that, rotor of SRM has no windings or permanent magnets which results in relative low copper losses, high robustness and low maintenance. Researchers are attracted to develop and improve the performance of SRM. Luan Ru presented a new structure of SRM stator in order to mitigate the drive vibration and noise by immersing the stator windings in an evaporative cooling medium [1]. M.A. Rahman and Kyohei Kiyota have developed a cylindrical rotor design for hybrid electric-vehicles [2]. Yu Hasegawa et al, presented a novel SRM using auxiliary permanent magnets on the stator yoke so as to increase the torque density [3]. Design modification, fabrication and performance analysis of 4-phases 8/6 SRM is given by D. Roy et al [4]. O. Argiolas et al proposed a drive design of 12/8 SRM with optimized geometry for torque ripples minimization [5]. The goal of this paper is to propose a novel design, fabrication and control of doubly fed switched reluctance motor (DFSRM). In the proposed double excitation fed SRM, rotor of SRM is employed by installing copper windings on the rotor poles as well as the stator poles. Rotor and stator windings are excited from a DC supply in order to increase the developed electro-magnetic torque; thus increasing the output power of the drive and keeping the system compactness. Also, a control strategy for the excitation of rotor and stator windings is presented. Performance analysis of the proposed SRM is carried out through Finite Element Methods Magnetics (FEMM) and MATLAB software. The novel doubly fed SRM and the control circuit are practically implemented and tested in laboratory for results validation.

This paper presents a novel Switched Reluctance Motor (SRM) design and implementation. Due to low manufacturing cost, cage-less rotor and wide speed range; SRM drive is used in many applications such as robotics, electric vehicles and aerospace industries. In this paper, rotor of SRM is employed by mounting copper windings on the rotor poles as well as the stator poles. Rotor and stator windings are excited from DC supply in order to increase the developed electro-magnetic torque; thus enhancing the output power of the drive and keeping the system compactness. Furthermore, the proposed SRM offers higher reliability than conventional one, if excitation of rotor windings is lost, the drive will turn into a conventional SRM, the drive will continue running as a conventional SRM. Finite element method magnetics (FEMM) software is applied to obtain the magnetic characteristics of the proposed SRM. A control strategy for excitation of rotor and stator windings is presented. MATLAB/Simulink modeling of the proposed SRM is given and validated by practical experiment. Experimental Results show that the proposed SRM is capable of achieving an increased torque compared with conventional SRM drive.

II. Basic Principles of Conventional SRM

SRM drive consists of an unequal number of salient rotor and stator poles. Coils are carried by the stator while the rotor is cage-less and has no magnets. Operation of conventional SRM depends on variable reluctance resultant in the air gap between the stator and rotor. There are famous stator-rotor (*ns/nr*) combination such as 6/4, 8/6 and 10/8 where *ns* is number of stator poles, *nr* is number of rotor poles. A driving converter is used as an interface between the DC supply and the SRM.

Manuscript was submitted for review on 19, October, 2018.
Eid Gouda, and M. Salah H. are with the Electrical Engineering Department, Faculty of Engineering, Mansoura University ,35516, Egypt.(e-mail: eid.gouda@yahoo.fr, mohamed.salah.wassif@gmail.com)
Digital Object Identifier 10.30941/CESTEMS.2019.00014

Circuit diagram of 6/4 SRM drive and the driver converter is shown in Fig. 1. each phase is excited through two transistors, two freewheeling diodes are used to return the stored magnetic energy in the coils back to the source.

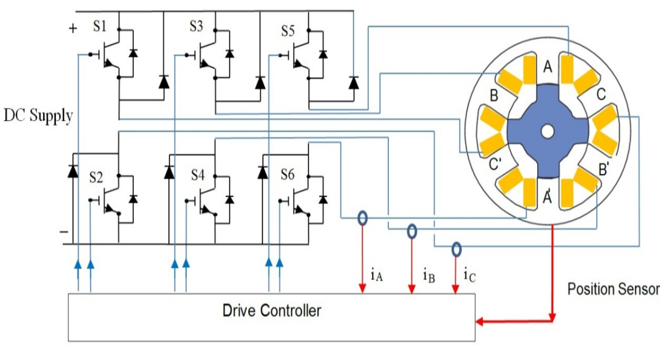

Fig. 1. Circuit diagram of 6/4 SRM drive system.

SRM drive has four operation quadrant for motoring and generating, selection of turn on and turn off angles defines the desired quadrant of operation as shown in Fig. 2.There Inductance pattern, torque profile and flux linkage for conventional SRM are shown in Fig. 3 at currents range from 1 to 50 A.

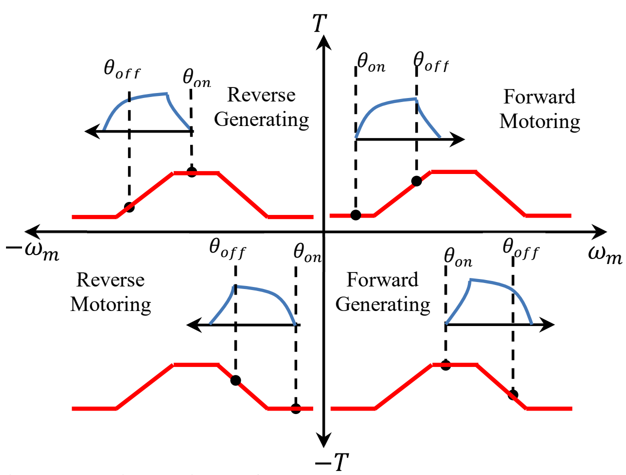

Fig. 2. Operation quadrants of SRM drive.

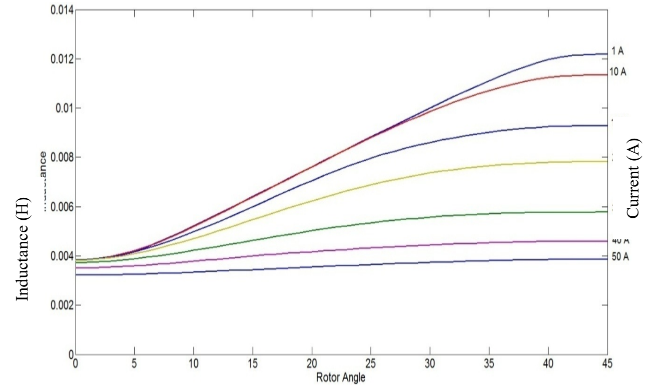

(a)

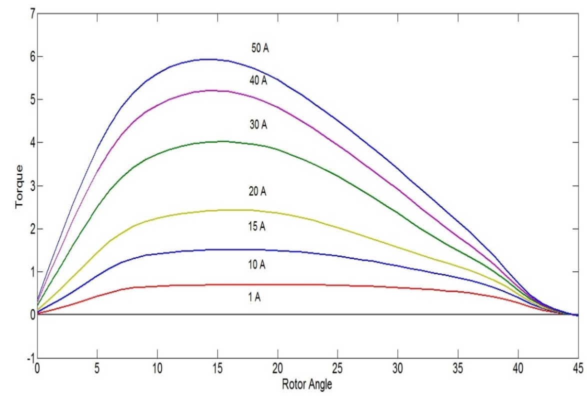

(b)

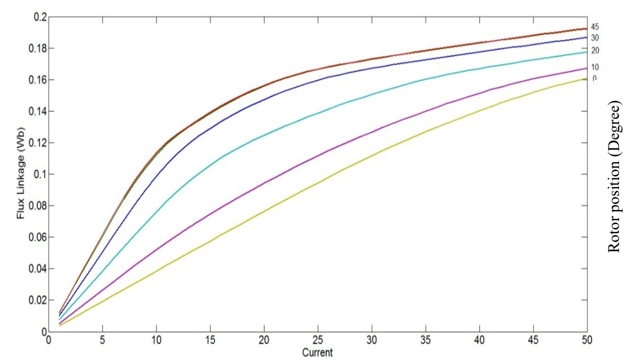

(c)

Fig. 3. (a) Inductance pattern, (b) Torque profile, and (c) Flux linkage.

III. Proposed Design of Doubly-Fed SRM (DFSRM)

Schematic structure of the proposed doubly fed SRM is shown in Fig.4. In the proposed doubly fed SRM, space of the rotor poles is employed by installing copper auxiliary windings on the rotor poles as well as the stator main windings. Rotor auxiliary windings are mounted in order to increase the developed electro-magnetic torque of the drive; thus enhancing the output power of the drive. Compared with conventional SRM, output power of the proposed doubly fed SRM is much higher at the same drive volume. Slip rings installed on the rotor shaft in order to supply dc power to rotor coils. Fixed carbon brushes are used to carry the electric current to the movable rings. Each two opposite poles of the rotor are connected in series as on coil. Energizing the rotor coils is executed through a control circuit in order to keep the polarity of rotor poles field compatible with the stator poles field.

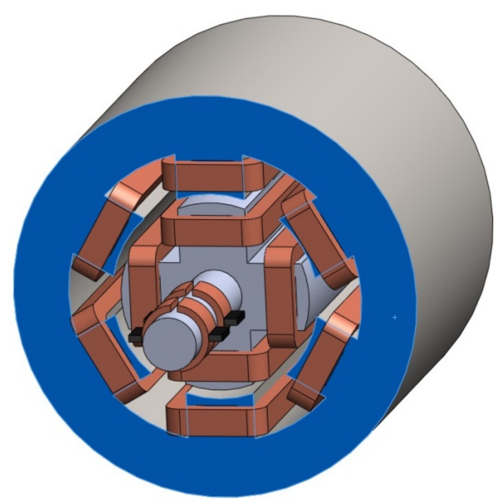

Fig. 4. Schematic structure of the proposed doubly fed SRM.

IV. Control Principles of Doubly-Fed SRM (DFSRM)

in the classical SRM drive, a rotor position sensor is used to control the turn on angle θ_{on} and the conduction angle θ_{Cond} of each phase switches, thus controlling the energizing of each phase of the SRM drive. In the proposed doubly fed SRM, the rotor position sensor is used to control energizing both of stator and rotor windings. slip ring is employed on the rotor shaft in order to connect power to the rotor coils. It can be noticed that the slip ring is split so as to reverse the current direction through the rotor coils.One complete cycle rotation of the proposed doubly fed SRM can be described as follows,

In Fig. 5 –a poles *E-E'* is aligned with *C-C'*; current is released to energize poles *A - D'* as north and *A'- D* as south.

In Fig. 5 –b poles *D-D'* is aligned with *A-A'*; current is released to energize poles B - E' as north and B'-E as south.

In Fig. 5 –c poles E-E' is aligned with B-B'; current is released to energize poles C-D' as north and C'-D as south.

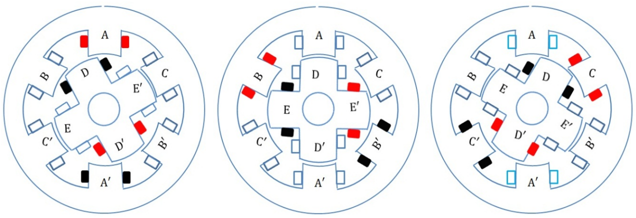

(a) (b) (c)

Fig. 5. Energizing poles (a) A-D'as north and A'-D as south, (b) B-E'as north and B'-E as south, (c) C-D'as north and C'-D as south.

In Fig. 6-a poles D-D' is aligned with C-C'; current is released to energize poles A –E' as north and A'-E as south pole.

In Fig. 6-b poles E-E' is aligned with A-A'; current is released to energize poles B-D as north pole and B'-D' as south pole, In Fig. 6-c poles D-D' is aligned with B-B'; current is released to energize poles C-E' as north pole and C'-E as south pole.

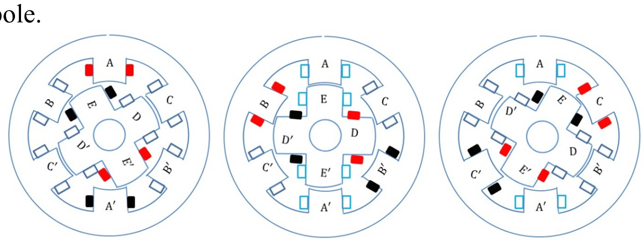

(a) (b) (c)

Fig. 6. Energizing poles (a) A-E'as north and A'-E as south, (b) B-Das north and B'-D' as south, (c) C-E'as north and C'-E as south.

In Fig. 7-a poles E-E' is aligned with C-C'; current is released to energize poles A-D as north and A' –D' as south pole. In Fig.7-b poles D-D' is aligned with A-A'; current is released to energize poles B –E as north pole and B'-E' as south pole. In Fig. 7-c poles E-E' is aligned with B-B'; current is released to energize poles C-D as north pole and C'-D' as south pole.

In Fig. 8-a poles D-D' is aligned with C-C'; current is released to energize stator poles A-E as north pole and A'-E' as south pole. In Fig. 8-b poles E-E' is aligned with A-A'; current is released to energize poles B-D' as north pole and B'-D as south pole. In Fig. 8-c poles D-D' is aligned with B-B'; current is released to energize poles C-E as north pole and C'-E' as south pole.

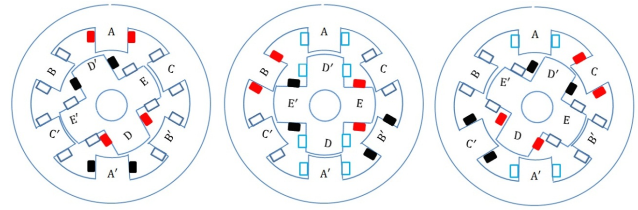

(a) (b) (c)

Fig. 7. Energizing poles (a) A-Das north and A'-D' as south, (b) B-E as north and B'-E' as south, (c) C-Das north and C'-D' as south.

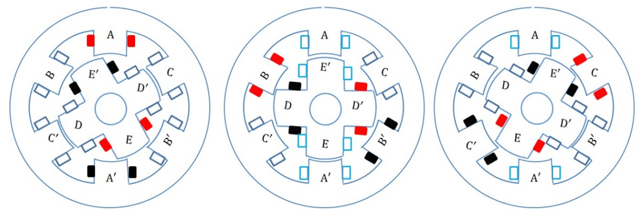

(a) (b) (c)

Fig. 8. Energizing poles (a) A-E as north and A'-E' as south, (b) B-D' as north and B'-D as south, (c) C-Eas north and C'-E' as south.

It can be noticed that the polarity of rotor poles is decided based on the stator poles polarity. Stator poles A, B or C are always north, while A', B' or C' are always south poles when energized. On the other hand, polarity of any of the rotor poles is decided based on the stator poles polarity. Rotor poles D, D', E or E' is north when any of these poles is about to get aligned with A', B' or C', and south when any of the rotor poles is about to get aligned with A, B or C. Fig. 9 shows control circuit for rotor windings which is supplied through carbon brushes and slip rings mounted on the rotor shaft.

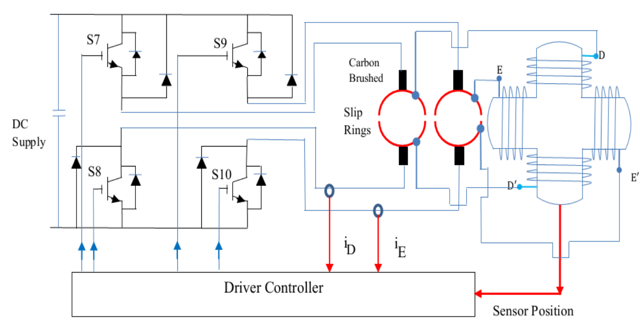

Fig. 9. Control circuit of rotor windings

V. Mathematical Analysis of DFSRM

Generally, differential input electrical energy = differential output mechanical energy + differential stored field energy + differential losses energy

For the proposed doubly excited SRM, the differential electrical energy supplied to the drive per single phase is given as follows:

$$dw_{ele} = i.d\psi \tag{1}$$

$$dw_{elec} = i_s.d\psi_s + i_r.d\psi_r \tag{2}$$

$$\psi_s = L_s.i_s + M.i_r \tag{3}$$

$$\psi_r = L_r.i_r + M.i_s \tag{4}$$

Substituting from (3) and (5.4) in (2):

$$dw_{ele} = i_s\,.\,L_s di_s + i_s{}^2 dL_s + i_s\,.\,M di_r + i_s\,.\,i_r dM + i_r\,.\,L_r di_r + i_r{}^2 dL_r + i_s\,.\,i_r dM \tag{5}$$

Form equation (4.5), differential Stored magnetic field energy, mechanical energy and resultant torque can be calculated form equation (4.5) as follows:

$$dw_{field} = \frac{1}{2} i_s{}^2 dL_s + i_s\,.\,L_s di_s + \frac{1}{2} i_r{}^2 dL_r + i_r\,.\,L_r di_r + i_s\,.\,M di_r + i_r\,.\,M di_s + i_s\,.\,i_r dM \tag{6}$$

$$dw_{mech} = T_{elec}.\,d\theta_r = dw_{elec} - dw_{field} = \frac{1}{2} i_s{}^2 dL_s + \frac{1}{2} i_r{}^2 dL_r + i_s\,.\,i_r dM \tag{7}$$

$$T_{elec} = \frac{1}{2} i_s{}^2 \frac{dL_s}{d\theta_r} + \frac{1}{2} i_r{}^2 \frac{dL_r}{d\theta_r} + i_s\,.\,i_r \frac{dM}{d\theta_r} \tag{8}$$

VI. Magnetic Analysis of DFSRM

Finite element method magnetics (FEMM) software is used for electro-magnetic analysis [6]. It's used to investigate the performance of the proposed doubly excited SRM at rotor angle θ from 0^0 (fully unaligned) to 45^0 (fully aligned) at stator excitation currents ranging from 0 to 50 A. Distribution of the flux density is shown in Fig10. Furthermore, flux lines of the rotor at different position is shown in Fig.11. Fig 12 shows the static torque profile of the drive phase (A) at excited stator currents from 0 to 50 A, when the rotor current is 0 A, in this case the drive acts as a conventional SRM. Fig. 13 shows the static torque profile of phase (A) of the proposed drive when the rotor current is 50% of the stator current. In this case, the drive torque has increased by 45%. Fig. 14 shows the static torque profile of phase (A) of the proposed drive when the rotor current is 100% of the stator current. In this case, the drive torque has increased by 75%.

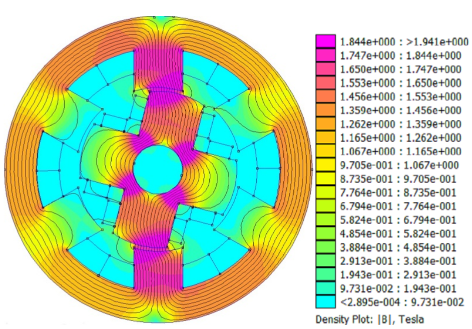

Fig. 10. Flux density destribution.

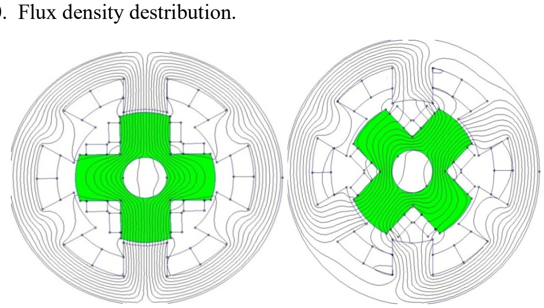

(a) (b)

Fig. 11. Rotor position (a) Fully aligned (b) Un-aligned.

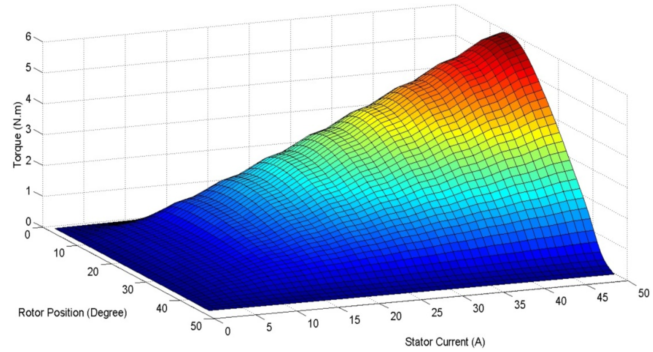

Fig. 12. Phase torque profile at *Ir=0*.

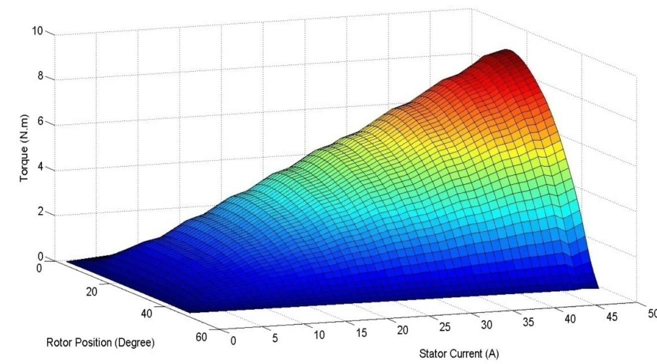

Fig. 13. Phase torque profile at *Ir=50% Is*.

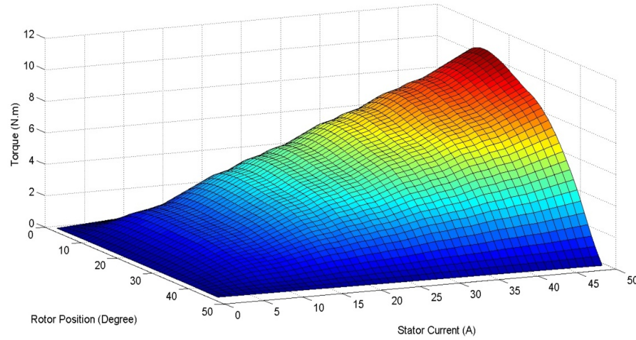

Fig. 14. Phase torque profile at *Ir=Is*.

Closed loop speed control block diagram of the modified doubly excited SRM is shown in Fig.15. The measured speed of the drive is compared with the reference speed through the speed controller. The speed controller generates a current signal that is compared with drive measured current. The error current is converted into a value of duty cycle through pulse width modulation (PWM) controller. Driver converter switches (stator and rotor) is controlled by PWM signals.

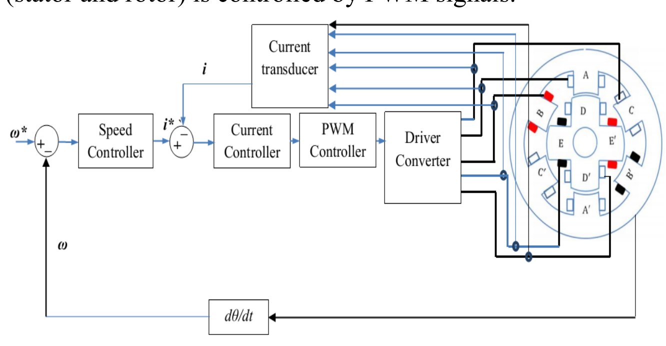

Fig. 15. Closed loop control of proposed doubly fed SRM

VII. Experimental Validation

Rotor of SRM is employed by installing copper windings on the rotor poles as well as the stator poles as shown in Fig 16. Rotor and stator windings are excited from a DC supply in order to increase the developed electro-magnetic torque; thus increasing the output power of the drive and keeping the system compactness.

Fig. 16 Installed windings on the rotor poles

Slip rings are installed on the rotor shaft in order to supply dc power to the rotor coils. Fixed carbon brushes are used to carry the electric current to the movable rings as shown in Fig 17. Each two opposite poles of the rotor are connected in series as on coil. Energizing the rotor coils is executed through a control circuit in order to keep the polarity of rotor poles field compatible with the stator poles field.

Fig. 17. Installed slip rings and carbon brushes on rortor shaft.

Fig 18 shows the DFSRM drive hardware control circuit and the experimental rig for obtaining static torque profile of the doubly fed SRM drive. Profile of the static torque is measured for one phase over a range of angular displacement [0^0 to 45^0] at 5A and 10A of DC current. The drive rotor is blocked with a fixed shaft; the shaft weight is measured by a weight measuring device. Given information of blocking shaft (*L= 40 cm*) and acceleration of gravity (*g= 9.81 m/S*^{2}), the resultant measured weight is then converted into static torque (*N.m*). The Profile of the static torque as a function of current and angular displacement is shown in Fig. 19.

Differences in results between simulated and calculated static torque of the doubly excited SRM is due to several reasons;

1. Error in the measuring units and in accurate weight to torque conversion,

2. Inaccurate measuring of the rotor dimensions used in FEMM, and

3. After adding coils to the rotor shaft, the drive became highly saturated.

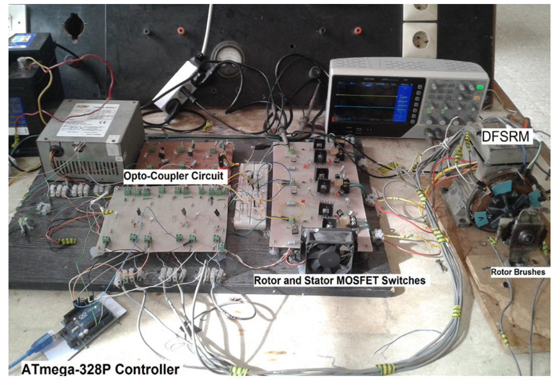

(a) DFSRM drive hardware control circuit

(b) static torque measurement.

Fig. 18. Experimental rig

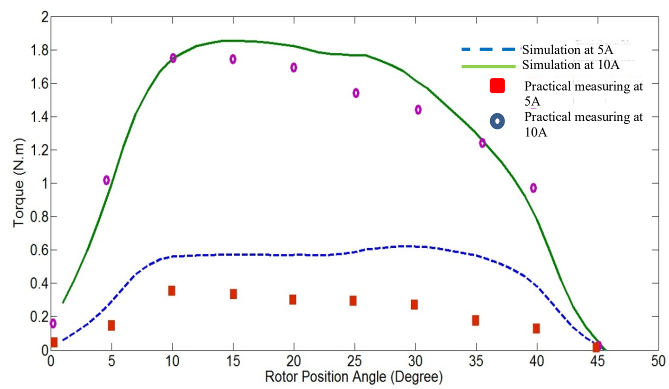

Fig. 19. Calculated and measured static torque at 5A and 10A for the proposed drive.

Stator and rotor currents of the proposed DFSRM is indicated in Fig 20. Although the applied DC voltage to stator and rotor control circuits are the same, currents of the rotor are lower than the stator currents due to the resistance of the carbon brushes and slip rings. The proposed drive presents higher torque density, but the cost is increased due to the installed windings on the rotor and complex control circuit. In addition to that, the need for carbon brushes and slip rings increased the cost as well as the need for maintenance.

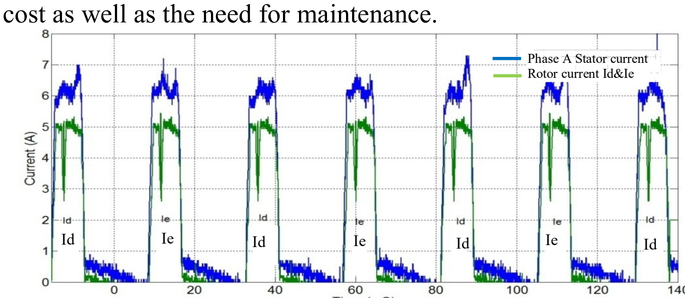

(a)

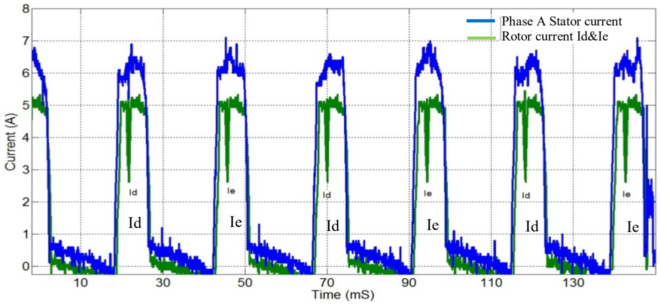

(b)

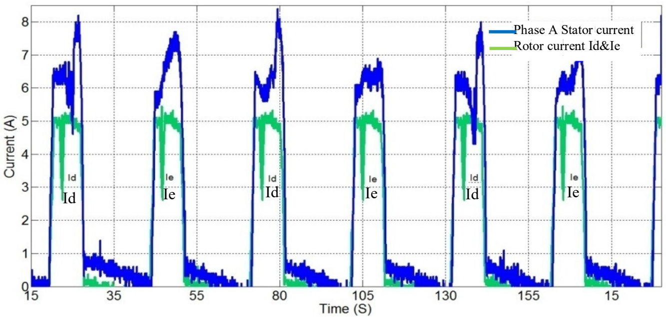

(c)

Fig. 20. Currents of the Doubly-Fed SRM (a) Phase a (a) Phase b, and (b) phase c.

As SRM can be used in high speed applications; In this case, a high quality slip rings should be used so as to bear the frictions forces with carbon brushes. In addition, the proposed drive will need a periodical maintenance plan to check up the slip rings and the carbon brushes health. Table 1 presents the performance parameters of conventional and doubly-fed SRM drive.

TABLE I
PARAMETERS OF CONVENTIONAL AND DOUBLY-FED SRM DRIVE.

Parameters	Conventional SRM	Doubly-fed SRM
Stator Poles	6	6
Rotor Poles	4	4
Rotor Windings	Not Applied	Applied
Power (W)	350	640
Efficiency (%)	82%	85%
Speed (rpm)	800	930

VIII. CONCLUSION

A novel design, fabrication and control of doubly fed switched reluctance motor were presented in this thesis. In the proposed double excitation fed SRM, rotor of SRM was employed by installing copper windings on the rotor poles as well as the stator poles. Rotor and stator windings are excited from a DC supply in order to increase the developed electro-magnetic torque; thus increasing the output power of the drive and keeping the system compactness. Also, a control strategy for the excitation of rotor and stator windings was presented. Performance analysis of the proposed SRM was carried out through FEMM and Matlab software.

Experimental test was carried out in order to validate results of the novel doubly fed SRM drive. Results showed that the torque density of the drive was increased at the same size of the drive. Although, the proposed drive has higher torque density, but the cost increased due to the installed windings on the rotor and the control circuit became more complex. In addition to that, the need for carbon brushes and slip rings increased the cost as well as the need for maintenance.

REFERENCES

[1] Luan Ru, "New Stator Structure Reducing Vibration and Noise in Switched Reluctance Motor" *2015 Eighteenth* International Conference on Electrical Machines and Systems (ICEMS), Oct. 25-28, 2015

[2] M.A. Rahman, KyoheiKiyota, Takeo Kakishima, Akira Chiba, "Cylindrical Rotor Design for Acoustic Noise and Windage Loss Reduction in Switched Reluctance Motor for HEV Applications", *IEEE Transactions on Industry Applications*, 2015

[3] Yu Hasegawa, Kenji Nakamura, and Osamu Ichinokura, "A Novel Switched Reluctance Motor with the Auxiliary Windings and Permanent Magnets", IEEE Transaction on Magnetics, Vol. 48, No. 11, November 2012.

[4] D. Roy, S. Mainuddin and M. Sengupta, "Design, analysis, FEM validation and fabrication of a switched reluctance motor," 2017 National Power Electronics Conference (NPEC), Pune, India, 2017, pp. 160-165.

[5] O. Argiolas, E. Nazeraj, O. Hegazy, J. De Backer, A. Mohammadi and J. Van Mierlo, "Design optimization of a 12/8 Switched Reluctance Motor for electric and hybrid vehicles," 2017 Twelfth International Conference on Ecological Vehicles and Renewable Energies (EVER), Monte Carlo, 2017, pp. 1-10.

[6] D. C. Meeker, Finite Element Method Magnetics, Version 4.2 (02 Nov. 2009 Build), http:// www.femm.info.

Eid Gouda was born in Arab Republic of Egypt in 1975. He received the B.S. and MSc degrees in electrical engineering from Mansoura University, Egypt in 1997 and 2004 respectively. At 2011 he earned his PhD in electrical engineering from Nancy-Universite, Faculte Des Sciences Et Technologies, France. In 2017, he became an associate Professor in electrical engineering at Mansoura University. His research interests include electrical machine analysis, electrical drives, power electronics and renewable energy.

Mohamed Salah was born in Arab Republic of Egypt in 1987. He received the B.S. and MSc degrees in electrical engineering from Mansoura University in 2008 and 2018 respectively. He is currently working in Thermal Power Station in Egypt as an operator engineer since 2012. His research interests include electrical machine analysis, electrical drives, power electronics and renewable energy. Currently, he is a PhD student at Mansoura University, faculty of engineering, at the department of electrical power.